An innovative micromechanics-based three-dimensional long-term strength criterion for fracture assessment of rock materials

Xiao-Ping Zhou, Xiao-Cheng Huang
School of Civil Engineering, Chongqing University, Chongqing 400045, China
State Key Laboratory of Coal Mine Disaster Dynamics and Control, Chongqing University, Chongqing 400044, China

Filippo Berto
Department of Mechanical Engineering, Norwegian University of Science and Technology, Trondheim 7491, Norway

ABSTRACT. Rocks may exhibit time-dependent behaviors. Long-term strength criterion significantly dominates creep failure of rocks. Rocks contain many microcracks, which lead to degrade of long-term strength. In this paper, it is assumed that there exist three-dimensional penny-shaped microcracks in rocks. The mode II stress intensity factors at tips of three-dimensional penny-shaped microcracks in Burgers viscoelastic rock matrix is derived. A novel micromechanics-based three-dimensional long-term strength criterion is established to consider the effects of time and the intermediate principal stress on creep failure of rocks. By comparison with the previous experimental data, it is found that the novel micromechanics-based three-dimensional long-term strength criterion is in good agreement with the experimental data.

KEYWORDS. Micromechanics-based three-dimensional long-term strength criterion; Burgers viscoelastic rock matrix; three-dimensional penny-shaped creep microcracks; Stress intensity factor; The intermediate principal stress.

OPEN ACCESS

Citation: Zhou, X.-P., Huang, X.-C., Berto, F., An innovative micromechanics-based three-dimensional long-term strength criterion for fracture assessment of rock materials, Frattura ed Integrità Strutturale, 44 (2018) 64-81.

Received: 19.01.2018
Accepted: 05.02.2018
Published: 01.04.2018

INTRODUCTION

In the past several decades or more, extensive laboratory creep experiments were conducted to study the creep behaviors of many kinds of rocks [1-5]. It is indicated that deformation of rocks under a constant load over extended a period of time generally exhibits primary or transient creep, lately by secondary or steady-rate creep, followed terminating in tertiary or accelerating creep that eventually progresses to dynamic rupture. Moreover, it is observed from laboratory creep experiments that the failure of rocks occurs at stresses well below the peak strength of rocks. Analyses that the short-term strength is applied to estimate the stability of the surrounding rock mass around tunnels have often predicted stable openings even though the failure of rock mass is observed in situ. For example, it is observed that the long-term strength of rock in situ can be as low as 50% of the short-term strength [6].

To investigate the long-term strength of rock, some long-term strength criteria of rocks were established to study the creep behaviors of rocks, such as Mises-Schleicher &Drucker-Prager unified(MSDPu) criterion, and so on. However, these long-term strength criteria were established using phenomenological approaches, which can produce the macroscopically observed creep curves of rocks by fitting with experimental data, and the inherent physical mechanisms related to time-dependent behaviors are not accommodated in these models, so the key mechanistic parameters remain physically unclear [7]. To authors' knowledge, three-dimensional long-term strength criterion of rocks, in which the effects of the intermediate principal stress are considered, is not proposed by using micromechanical methods. In fact, rock is a kind of discontinuity medium containing many microcracks and microdefects, the presence of such microcracks strongly influences the macroscopic mechanical behavior of rocks by serving as stress concentrators and leading to microcracking [8-12].

To overcome the disadvantages encountered in phenomenological models, it is necessary to study the effects of initiation and propagation of microcracks and microdefects on the creep failure of rocks. In this paper, micromechanical methods are used to investigate the lone-term strength of rocks. Moreover, a novel micromechanics–based three-dimensional nonlinear long-term strength criterion is established to study the effects of time and the intermediate principal stress on the creep failure of rocks. By comparison with experimental data, it is found that the novel micromechanics–based three-dimensional long-term strength criterion is in good agreement with the experimental data.

THE ANALYTICAL MODEL

It is generally accepted that the creep deformation and fracturing process that evolve in rocks are closely related to the intrinsic property and stress condition of rocks, such as fracture toughness, internal frictional angle, the dip and orientation angle of microcracks, Poisson's ratio, and so on. In this paper, it is assumed that the creep failure of rocks is due to the presence of penny-shaped microcracks and there is abundant evidence for the existence of microcracks in rocks [13-14]. Therefore, this model is physically plausible and the following assumptions are made: (i) penny-shaped microcracks are assumed to be randomly distributed in Burgers viscoelastic rock matrix; (ii) the interaction between penny-shaped microcracks is neglected before the coalescence of microcracks.

Stress intensity factor of penny-shaped microcracks embedded in Burgers viscoelastic rock matrix

It is assumed that the tensile stress is negative, and the compressive stress is positive. Consider a single penny-shaped creep microcrack in Burgers viscoelastic rock matrix uniformly loaded at far field. Establish a global coordinate system ($O-x_1x_2x_3$.) and its corresponding local coordinate system ($O-x_1'x_2'x_3'$), as shown in Fig. 1. In a global coordinate system ($O-x_1x_2x_3$), the direction of the maximum principal stress is parallel to the x_1-axis, the direction of the intermediate principal stress is parallel to the x_2-axis, the direction of the minimum principal stress is parallel to the x_3-axis. In the local coordinate system ($O-x_1'x_2'x_3'$), the direction of the x_2'-axis is parallel to the normal direction of penny–shaped creep microcrack. The angle between the x_2'-axis and the x_2-axis is the dip angle of penny–shaped creep microcrack θ. The angle between the x_3'-axis and the x_3-axis is the orientation angle of penny–shaped creep microcrack φ.

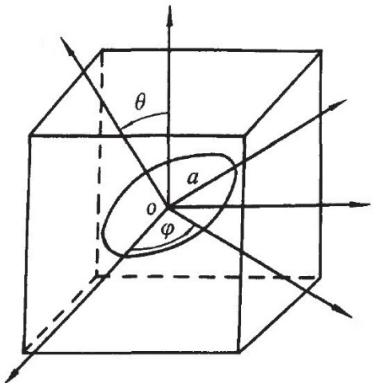

Figure 1: Mechanical model for penny-shaped microcrack embedded by Burgers viscoelastic rock matrix.

The stresses in the local coordinate system are given by Yu and Feng [15],

$$\sigma'_{ij} = g'_{ik} g'_{jl} \sigma_{kl} \tag{1}$$

where,

$$g'_{ij} = \begin{bmatrix} \cos\theta\cos\varphi & \sin\theta & -\cos\theta\sin\varphi \\ -\sin\theta\cos\varphi & \cos\theta & \sin\theta\sin\varphi \\ \sin\varphi & 0 & \cos\varphi \end{bmatrix} \tag{2}$$

Then, σ'_{22} , σ'_{21} and σ'_{23} can be respectively expressed as follows:

$$\begin{cases} \sigma'_{22} = \sigma_1 \sin^2\theta\cos^2\varphi + \sigma_2 \cos^2\theta + \sigma_3 \sin^2\theta\sin^2\varphi \\ \sigma'_{21} = \sigma_2 \sin\theta\cos\theta - \sigma_1 \sin\theta\cos\theta\cos^2\varphi - \sigma_3 \sin\theta\cos\theta\sin^2\varphi \\ \sigma'_{23} = \sigma_3 \sin\theta\sin\varphi\cos\varphi - \sigma_1 \sin\theta\sin\varphi\cos\varphi \end{cases} \tag{3}$$

Yu and Feng [15] and Tada [16] defined the stress intensity factors at tips of penny-shaped microcracks embedded in isotropic and elastic rock matrix as

$$K_{II} = \frac{4\left[\sqrt{\left(\sigma'_{21}\right)^2 + \left(\sigma'_{23}\right)^2} - \mu\left(\sigma'_{22}\right)\right]}{2-\nu}\sqrt{\frac{a}{\pi}} \tag{4}$$

where μ is the frictional coefficient on the crack surfaces, ν is Poisson's ratio, K_{II} is the mode II stress intensity factor.

The Burgers creep model

In this paper, it is assumed that microcracks are embedded in Burgers viscoelastic rock matrix with the characteristic of instantaneous elastic deformation, primary creep and steady-rate creep.

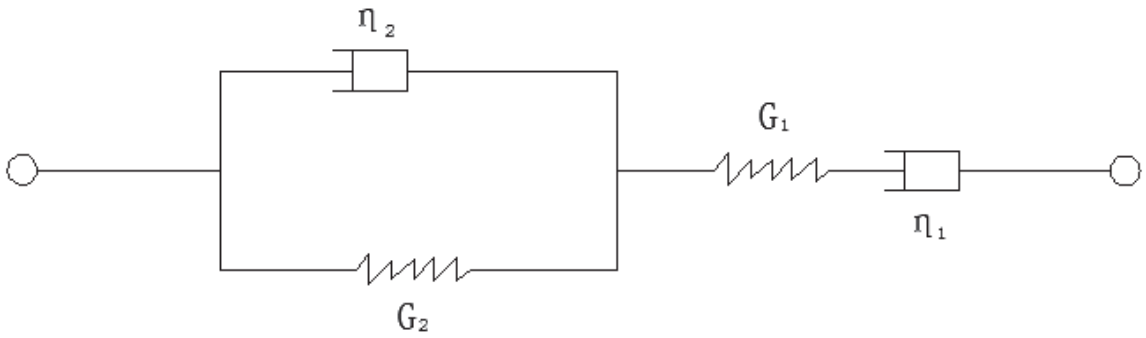

Figure 2: The diagram of Burgers model.

As shown in Fig. 2, Burgers model can be expressed as follows

$$e''_{ij} + \frac{G_2}{\eta_2} e'_{ij} = \frac{1}{2G_1} S_{ij} + \left(\frac{1}{2\eta_2} + \frac{1}{2\eta_1} + \frac{G_2}{2G_1\eta_2}\right) S'_{ij} + \frac{G_2}{2\eta_1\eta_2} S''_{ij} \tag{5}$$

where G_1 is Maxwell shear modulus, G_2 is Kelvin shear modulus, η_1 is Maxwell viscosity, and η_2 is Kelvin viscosity, $S_{ij}=\sigma_{ij}-\frac{\delta_{ij}}{3}(\sigma_{11}+\sigma_{22}+\sigma_{33})$, $e_{ij}=\varepsilon_{ij}-\frac{\delta_{ij}}{3}(\varepsilon_{11}+\varepsilon_{22}+\varepsilon_{33})$, $\delta_{ij}=\begin{cases}1 & i=j\\ 0 & i\neq j\end{cases}$, σ_{ij} is stress tensor, ε_{ij} is strain tensor. The Maxwell shear modulus is equal to elasticity shear modulus, $e''_{ij}=\frac{d^2e_{ij}}{dt^2}$, $e'_{ij}=\frac{de_{ij}}{dt}$, $S''_{ij}=\frac{d^2S_{ij}}{dt^2}$, $S'_{ij}=\frac{dS_{ij}}{dt}$.

Eq.(5) can be rewritten as

$$e_{ij}=S_{ij}\left[\frac{1}{2G_1}+\frac{t}{2\eta_1}+\frac{1}{2G_2}\left(1-e^{\frac{G_2}{\eta_2}t}\right)\right] \tag{6}$$

where t is the creep time.

From Eq.(6) and works by Yi and Zhu [17], the time factor of the Burgers model under a given load is obtained as

$$\begin{cases}f_{i\sigma}(t)=H(t)\\ f_{iu}(t)=1+\frac{G_1}{\eta_1}t+\frac{G_1}{G_2}\left[1-\exp\left(-\frac{G_2}{\eta_2}t\right)\right]\end{cases} \tag{7}$$

where $f_{iu}(t)$ is the time factor for displacement, $f_{i\sigma}(t)$ is the time factor for stress, $H(t)=\begin{cases}1, t\geq 0\\ 0, t<0\end{cases}$ is Heaviside function.

According to works by Zhou [18], energy release rate at tips of the mixed mode I- II-III microcracks in Burgers viscoelastic rock matrix can be written as

$$G(t)=G_I(t)+G_{II}(t)+G_{III}(t)=\frac{1-v^2}{E}(K_I^2+{K_{II}}^2+\frac{1}{1-v}{K_{III}}^2)f_{iu}(t) \tag{8}$$

where

$$f_{iu}(t)=1+\frac{G_1}{\eta_1}t+\frac{G_1}{G_2}\left[1-\exp\left(-\frac{G_2}{\eta_2}t\right)\right].$$

In Eq. (8), $G(t)$ can be rewritten as

$$G(t)=f_{iu}(t)G \tag{9}$$

where G is energy release rate at tips of the mixed mode I-II-III microcracks in elastic rock matrix.

As for the creep fracture, the stress and displacement fields at tips of microcracks can be obtained as follows:

$$\begin{cases}\sigma_{ij}^{(m)}(t)=\sigma_{ij}^{(m)}\frac{K_m(t)}{K_m}\\ u_i^{(m)}(t)=u_i^{(m)}\frac{K_m(t)}{K_m}\end{cases} \tag{10}$$

where m =I, II and III, which are, respectively, denoted by mode I, II and III microcracks, $\sigma_{ij}^{(m)}$ and $u_i^{(m)}$ are, respectively, the stress and displacement fields at tips of microcracks in elastic rock matrix, $\sigma_{ij}^{(m)}(t)$ and $u_i^{(m)}(t)$ are, respectively, the stress and displacement fields at tips of microcracks in Burgers viscoelastic rock matrix, $K_m(t)$ and K_m are, respectively, stress intensity factor at tips of microcracks in Burgers viscoelastic and elastic rock matrix.
According to the definition of stress intensity factor, stress intensity factor at tips of microcracks can be denoted by

$$\begin{cases} K_m = \lim\limits_{x\to 0}\left[\sigma_{ij}^{(m)}\Big|_{y=0}\sqrt{2\pi x}\right] \\ K_m(t) = \lim\limits_{x\to 0}\left\{\sigma_{ij}^{(m)}(t)\Big|_{y=0}\sqrt{2\pi x}\right\} \end{cases} \tag{11}$$

Based on the definition of energy release rate, energy release rate at tips of microcracks can be defined by

$$G(t) = \lim_{\delta a\to 0}\frac{1}{\delta a}\int_0^{\delta a}\left[\sigma_{yy}(x,0)u_y(x-\delta a,0)+\sigma_{yx}(x,0)u_x(x-\delta a,0)+\sigma_{y\tilde{z}}(x,0)u_{\tilde{z}}(x-\delta a,0)\right]dx \tag{12}$$

where a is the growth length of microcracks.
Substituting Eq. (10) into Eq. (12) yields

$$\begin{aligned} G(t) &= \lim_{\delta a\to 0}\frac{1}{\delta a}\int_0^{\delta a}\left[\sigma_{ij}^{(m)}(t)u_i^{(m)}(t)\right]dx \\ &= \lim_{\delta a\to 0}\frac{1}{\delta a}\int_0^{\delta a}\left\{\sigma_{ij}^{(m)}\frac{K_m(t)}{K_m}\right\}\left\{u_i^{(m)}\frac{K_m(t)}{K_m}\right\}dx \\ &= \lim_{\delta a\to 0}\frac{1}{\delta a}\int_0^{\delta a}\left[\sigma_{ij}^{(m)}u_i^{(m)}\right]dx \\ &= \frac{\left[K_m(t)\right]^2}{\left(K_m\right)^2}G \end{aligned} \tag{13}$$

From Eq. (13) and Eq. (9), the stress intensity factors of creep cracks can be written as

$$K_m(t) = K_m\sqrt{\frac{G(t)}{G}} = K_m\sqrt{f_{iu}(t)} \tag{14}$$

For three-dimensional penny-shaped microcracks, frictional sliding is caused by the effective shear stress. As the effective shear force is greater than the frictional resistance along the slip surface, frictional slip would lead to the tensile stress at the two tips of the slip surface, which form the wing cracks, as shown in Fig. 3.
Substituting Eq. (4) into Eq. (14) yields:

$$K_{II} = \frac{4\sqrt{f_{iu}(t)}\left[\sqrt{\left(\sigma_{21}'\right)^2+\left(\sigma_{23}'\right)^2}-\mu\left(\sigma_{22}'\right)\right]}{2-\nu}\sqrt{\frac{a}{\pi}} \tag{15}$$

where μ is the frictional coefficient on the crack surfaces, ν is Poisson' s ratio, K_{II} is the mode II stress intensity factor, $f(t)$ denotes the time factor.
According to works by Tada [16], the condition of unstable growth of the mode II microcracks can be written as

$$K_{II}(t_0) = \kappa K_{IC} \tag{16}$$

where

$$\begin{cases}\sigma'_{22}=\sigma_1\sin^2\theta\cos^2\varphi+\sigma_2\cos^2\theta+\sigma_3\sin^2\theta\sin^2\varphi\\ \sigma'_{21}=\sigma_2\sin\theta\cos\theta-\sigma_1\sin\theta\cos\theta\cos^2\varphi-\sigma_3\sin\theta\cos\theta\sin^2\varphi\\ \sigma'_{23}=\sigma_3\sin\theta\sin\varphi\cos\varphi-\sigma_1\sin\theta\sin\varphi\cos\varphi\end{cases}$$

κ can be obtained from experimental results, or approximation suggested in the literature on the kinked crack, such as $\kappa=\sqrt{3}/2$ in the maximum-stress criterion [19], t_0 is the time of creep failure of microcracks, K_{IC} is toughness of rocks, which can be obtained by induced tensile strength and crack length, namely

$$K_{IC}=2\sigma_t\sqrt{\frac{a}{\pi}} \tag{17}$$

where σ_t is short-term uniaxial tensile strength of rocks.

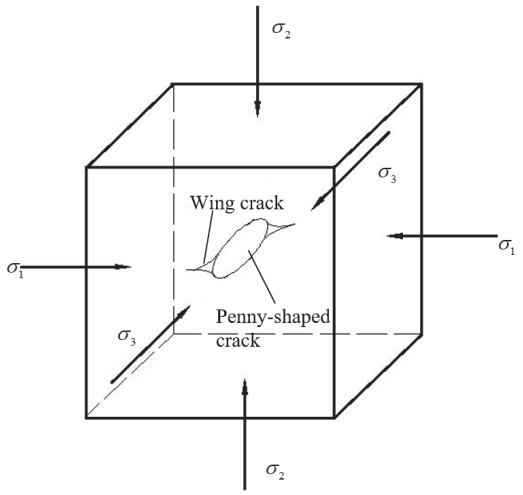

Figure 3: Propagation of wing cracks from the tip of penny-shaped microcrack.

THE ORIENTATION ANGLE OF MICRO-FAILURE IN ROCKS

It is generally accepted that the creep failure of rocks is induced by the fragment of large amounts of internal microcracks. However, it is very difficult to quantitatively analyze the number of microcracks. Therefore, micro-failure orientation angle α is introduced to define the number of propagating penny-shaped creepmicrocracks, as shown in Fig. 4. The fan-shaped area of wing crack distribution zone shown in Fig. 4 can be obtained from Eqs(15)-(16). The included angle of the fan section is denoted as the micro-failure orientation angle α. Substituting Eq.(15) into Eq.(16) yields:

$$\begin{aligned}&(\sigma_1-\sigma_3)^2(\mu^2-1)\sin^4\theta\cos^4\varphi+(\sigma_1-\sigma_3)\\&\sin^2\theta\left[2c\mu+2(\sigma_2-\sigma_3)\cos^2\theta+2\mu^2\left(\sigma_2\cos^2\theta+\sigma_3\sin^2\theta\right)-(\sigma_1-\sigma_3)\right]\cos^2\varphi\\&+\left\{-(\sigma_2-\sigma_3)^2\sin^2\theta\cos^2\theta+\left[c+\mu\left(\sigma_2\cos^2\theta+\sigma_3\sin^2\theta\right)\right]^2\right\}\le 0\end{aligned} \tag{18}$$

where $c=\frac{\kappa\sigma_t(2-\nu)}{2\sqrt{f_{iu}(t)}}$, σ_1 is the maximum principal stress, σ_2 is the intermediate principal stress, σ_3 is the minimum principal stress, the compressive stresses are defined to be positive in this paper.

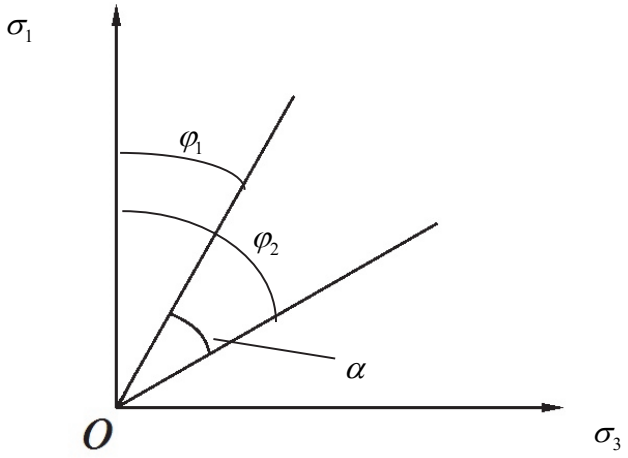

Figure 4: Wing crack distribution zone

Eq.(18) can be rewritten as :

$$C_1\cos^4\varphi+C_2\cos^2\varphi+C_3\le 0 \tag{19}$$

where

$$\begin{cases} C_1=(\sigma_1-\sigma_3)^2(\mu^2+1)\sin^4\theta \\ C_2=(\sigma_1-\sigma_3)\sin^2\theta\left[2c\mu+2\cos^2\theta\left(\mu^2+1\right)\sigma_2+2\left(\mu^2\sin^2\theta-\cos^2\theta\right)\sigma_3-(\sigma_1-\sigma_3)\right] \\ C_3=-(\sigma_2-\sigma_3)^2\sin^2\theta\cos^2\theta+\left[c+\mu\left(\sigma_2\cos^2\theta+\sigma_3\sin^2\theta\right)\right]^2 \end{cases}$$

From Eq. (19), the cosine of φ can be written as

$$\cos^2\varphi_1\le\cos^2\varphi\le\cos^2\varphi_2 \tag{20}$$

where

$$\begin{cases} \cos^2\varphi_1=\dfrac{-C_2+\sqrt{C_2^2-4C_1C_3}}{2C_1} \\ \cos^2\varphi_2=\dfrac{-C_2-\sqrt{C_2^2-4C_1C_3}}{2C_1} \end{cases}$$

From Eq.(20), supposing $\alpha=\varphi_2-\varphi_1$, the following equation can be written

$$\cos\alpha=\cos(\varphi_2-\varphi_1)=\cos\varphi_2\cos\varphi_1+\sin\varphi_2\sin\varphi_1 \tag{21}$$

CREEP FAILURE CHARACTERISTIC PARAMETERS OF ROCKS

The creep failure characteristic parameter of rocks should be constant when rocks entirely break. Damage mechanics reveals that the nucleation and initiation of microcracks does not imply creep failure of rock-like materials [20-22]. Many experiments show that the maximum principal stress should be further increased to assure that the wing crack continually propagates, while the minimum principal stress can significantly restrain wing crack to grow [23]. Therefore, the initiation of wing cracks cannot indicate creep failure of rocks. As a result, nucleation and initiation of internal microcracks cannot be chosen as the creep failure characteristic parameters.

The larger the minimum principal stress, the smaller the micro-failure orientation angle α. The micro-failure orientation angle α does not keep constant, $\tan\alpha$, $\sin\alpha$ and $\cos\alpha$ do not also keep constant. Therefore, the micro-failure orientation angle α, $\tan\alpha$, $\sin\alpha$ and $\cos\alpha$ cannot be considered as the creep failure characteristic parameters.

Microcracks randomly distribute in Burgers viscoelastic rock matrix, and the orientation angle of each microcrack randomly distributes. Therefore, the micro-failure orientation angle α can be adopted to investigate the micro-failure density. An increase in the minimum principal stress leads to a decrease in the micro-failure density. The internal micro-failure density does not keep constant. Therefore, the micro-failure density cannot also be chosen as the creep failure characteristic parameters.

Reference [24] suggested that the creep failure of rocks occurs when the volumetric strain due to the internal micro-failure density reaches a critical value. Therefore, the creep failure characteristic parameters of rocks should be relevant to the internal micro-failure density, which is related to the micro-failure orientation angle α. Moreover, the creep failure characteristic parameters should satisfy the following three principles: firstly, the expression of the creep failure characteristic parameter should be in a simple mathematic one; secondly, the higher the minimum principal stress, the lower the micro-failure orientation angle; finally, the theoretical result should agree well with the experimental data.

Obviously, the expressions of the micro-failure orientation angle α, $\tan\alpha$ and $\sin\alpha$ are so complicated that it cannot be chosen as the creep failure characteristic parameters. Compared with the expressions of α, $\tan\alpha$ and $\sin\alpha$, the expression of $\cos\alpha$ is the simplest. The expression of $\sigma_1=\sigma_c$ is also the simplest Therefore, $\sigma_1=\sigma_c$ satisfies the first and second principles.

According to the second principle and Eq. (21), the cosine of the micro-failure orientation angle α can be expressed in following form:

$$\cos\alpha=\sqrt{\frac{C_3}{C_1}}+\sqrt{1+\frac{C_2}{C_1}+\frac{C_3}{C_1}} \tag{22}$$

where

$$\begin{cases} C_1=C_{11}\sigma^2 \\ C_2=C_{21}\sigma^2+C_{22}\sigma \\ C_3=-\left(\sigma_2-\sigma_3\right)^2\sin^2\theta\cos^2\theta+\left[c+\mu\left(\sigma_2\cos^2\theta+\sigma_3\sin^2\theta\right)\right]^2 \\ C_{11}=(\mu^2+1)\sin^4\theta \\ C_{21}=-\sin^2\theta \\ C_{22}=\sin^2\theta\left[2c\mu+2\cos^2\theta\left(\mu^2+1\right)\sigma_2+2\left(\mu^2\sin^2\theta-\cos^2\theta\right)\sigma_3\right] \\ \sigma=\sigma_1-\sigma_3 \end{cases}$$

It is indicated from Eq.(22) that the cosine of the micro-failure orientation angle increases with an increase in the minimum principal stress σ_3, while the micro-failure orientation angle α decreases with increasing the minimum principal stress σ_3.

For an invariable intermediate principal stress σ_2 and an invariable minimum principal stress σ_3, the relationship between $\cos\alpha$ and the maximum principal stress can be defined. Differentiating Eq. (22) with respect to σ_1 yields:

$$\left|\frac{\partial\cos\alpha}{\partial\sigma_1}\right|=\frac{1}{\sqrt{C_{11}}\sigma^2}\left(\sqrt{C_3}+\frac{C_{22}\sigma+2C_3}{2\sqrt{\left(C_{11}+C_{21}\right)\sigma^2+C_{22}\sigma+C_3}}\right) \tag{23}$$

where $\left|\frac{\partial\cos\alpha}{\partial\sigma_1}\right|$ is defined as the rate of change of $\cos\alpha$ to the maximum principal stress.

From Eq. (22), the maximum principal stress can be expressed as

$$\sigma=\sigma_1-\sigma_3=-\frac{2\cos\alpha\sqrt{C_{11}C_3}+C_{22}}{C_{21}+C_{11}\sin^2\alpha} \tag{24}$$

Substituting Eq. (24) into Eq. (23) yields

$$\left|\frac{\partial\cos\alpha}{\partial\sigma_1}\right|=\frac{\left(C_{21}+C_{11}\sin^2\alpha\right)^2}{\sqrt{C_{11}}\left(C_{22}+2\sqrt{C_{11}C_3}\cos\alpha\right)^2}$$
$$\left\{\sqrt{C_3}+\frac{-{C_{22}}^2-2C_{22}\sqrt{C_{11}C_3}\cos\alpha+2C_3\left(C_{21}+C_{11}\sin^2\alpha\right)}{2\sqrt{C_3+\left(C_{11}+C_{21}\right)\left(C_{22}+2\sqrt{C_{11}C_3}\cos\alpha\right)^2-C_{22}\left(C_{22}+2\sqrt{C_{11}C_3}\cos\alpha\right)\left(C_{21}+C_{11}\sin^2\alpha\right)}}\right\} \tag{25}$$

If the short-term uniaxial compressive strength of rocks is known, three-dimensional long-term strength criterion of rocks can be expressed by short-term uniaxial compressive strength of rocks. Therefore, for the short-term uniaxial compression condition $\sigma_1=\sigma_c$, $\sigma_2=0$, $\sigma_3=0$, we can obtain $\left|\partial\cos\alpha/\partial\sigma_1\right|$ at $t=0$ as,

$$\left|\frac{\partial\cos\alpha}{\partial\sigma_1}\right|=\frac{c_0}{{\sigma_c}^2\sqrt{\mu^2+1}}\left[\csc^2\theta+\frac{\mu\sigma_c+c_0\csc^2\theta}{\sqrt{\left(c_0+\mu\sigma_c\sin^2\theta\right)^2-{\sigma_c}^2\sin^2\theta\cos^2\theta}}\right] \tag{26}$$

where $c_0=\frac{\kappa\sigma_t(2-\nu)}{2\sqrt{f_{iu}(0)}}$, σ_c is the short-term uniaxial compressive strength of rocks, $f_{iu}(0)$ is the time factor when $t=0$.

Substituting Eq. (23) into Eq. (26) yields

$$\frac{1}{\sqrt{C_{11}}\sigma^2}\left(\sqrt{C_3}+\frac{C_{22}\sigma+2C_3}{2\sqrt{\left(C_{11}+C_{21}\right)\sigma^2+C_{22}\sigma+C_3}}\right)=$$
$$\frac{c_0}{{\sigma_c}^2\sqrt{\mu^2+1}}\left[\csc^2\theta+\frac{\mu\sigma_c+c_0\csc^2\theta}{\sqrt{\left(c_0+\mu\sigma_c\sin^2\theta\right)^2-{\sigma_c}^2\sin^2\theta\cos^2\theta}}\right] \tag{27}$$

From Eq. (27), three-dimensional long-term strength criterion expressed by the short-term uniaxial compressive strength of rocks can be denoted by

$$A_1\left(\sigma_1-\sigma_3\right)^4+A_2\left(\sigma_1-\sigma_3\right)^3+A_3\left(\sigma_1-\sigma_3\right)^2+A_4\left(\sigma_1-\sigma_3\right)+A_5=0 \tag{28}$$

where

$$\begin{cases} A_1=4C_{11}C_4^2\left(C_{11}+C_{21}\right) \\ A_2=4C_{11}C_{22}C_4^2 \\ A_3=4\left[C_{11}C_3C_4^2-2\left(C_{11}+C_{21}\right)C_4\sqrt{C_{11}C_3}\right] \\ A_4=-2C_{22}C_4\sqrt{C_{11}C_3} \\ A_5=4\left[C_3\left(C_{11}+C_{21}\right)-2C_3C_4\sqrt{C_{11}C_3}\right]-C_{22}^2 \\ C_{11}=(\mu^2+1)\sin^4\theta \\ C_{21}=-\sin^2\theta \\ C_{22}=\sin^2\theta\left[2c\mu+2\cos^2\theta\left(\mu^2+1\right)\sigma_2+2\left(\mu^2\sin^2\theta-\cos^2\theta\right)\sigma_3\right] \\ C_3=-\left(\sigma_2-\sigma_3\right)^2\sin^2\theta\cos^2\theta+\left[c+\mu\left(\sigma_2\cos^2\theta+\sigma_3\sin^2\theta\right)\right]^2 \\ C_4=\dfrac{c_0}{\sigma_c^{\,2}\sqrt{\mu^2+1}}\left[\csc^2\theta+\dfrac{\mu\sigma_c+c_0\csc^2\theta}{\sqrt{\left(c_0+\mu\sigma_c\sin^2\theta\right)^2-\sigma_c^{\,2}\sin^2\theta\cos^2\theta}}\right] \end{cases}$$

It is observed from Eq. (28) that $\left(\sigma_1-\sigma_3\right)$ is related to the friction coefficient μ, the coefficient κ of mixed-mode fracture criterion, the short-term uniaxial compressive strength σ_c, the short-term uniaxial tensile strength σ_t, the time factor $f_{iu}(0)$, the dip angle of penny-shaped microcracks θ and Poisson's ratio ν.

If the long-term uniaxial compressive strength of rocks is known, three-dimensional long-term strength criterion of rocks can be expressed by long-term uniaxial compressive strength of rocks. Therefore, for the long-term uniaxial compressive condition $\sigma_1=\sigma_{cl}$, $\sigma_2=0$, $\sigma_3=0$, we can obtain the rate of change constant $\left|\partial\cos\alpha/\partial\sigma_1\right|$ $\left|\partial\cos\alpha/\partial\sigma_1\right|$ at $t=t_0$ as,

$$\left|\frac{\partial\cos\alpha}{\partial\sigma_1}\right|=\frac{c_{t_0}}{\sigma_{cl}^{\,2}\sqrt{\mu^2+1}}\left[\csc^2\theta+\frac{\mu\sigma_{cl}+c_{t_0}\csc^2\theta}{\sqrt{\left(c_{t_0}+\mu\sigma_{cl}\sin^2\theta\right)^2-\sigma_{cl}^{\,2}\sin^2\theta\cos^2\theta}}\right] \tag{29}$$

where $c_{t_0}=\dfrac{\kappa\sigma_t(2-\nu)}{2\sqrt{f_{iu}(t_0)}}$, σ_{cl} is the long-term uniaxial compressive strength of rocks, $f_{iu}(t_0)$ is the time factor when $t=t_0$, t_0 is the time of creep failure of rocks under uniaxial compressive loads.

Substituting Eq. (29) into Eq. (23) yields:

$$\frac{1}{\sqrt{C_{11}}\sigma^2}\left(\sqrt{C_3}+\frac{C_{22}\sigma+2C_3}{2\sqrt{(C_{11}+C_{21})\sigma^2+C_{22}\sigma+C_3}}\right)= \\ =\frac{c_{t_0}}{{\sigma_{cl}}^2\sqrt{\mu^2+1}}\left[\csc^2\theta+\frac{\mu\sigma_{cl}+c_{t_0}\csc^2\theta}{\sqrt{\left(c_{t_0}+\mu\sigma_{cl}\sin^2\theta\right)^2-{\sigma_{cl}}^2\sin^2\theta\cos^2\theta}}\right] \tag{30}$$

From Eq. (30), micromechanics-based three-dimensional long-term strength criterion of rocks expressed by long-term uniaxial compressive strength of rocks can written as

$$A_1\left(\sigma_1-\sigma_3\right)^4+A_2\left(\sigma_1-\sigma_3\right)^3+A_3\left(\sigma_1-\sigma_3\right)^2+A_4\left(\sigma_1-\sigma_3\right)+A_5=0 \tag{31}$$

where

$$\begin{cases} A_1=4C_{11}C_4^2\left(C_{11}+C_{21}\right) \\ A_2=4C_{11}C_{22}C_4^2 \\ A_3=4\left[C_{11}C_3C_4^2-2\left(C_{11}+C_{21}\right)C_4\sqrt{C_{11}C_3}\right] \\ A_4=-2C_{22}C_4\sqrt{C_{11}C_3} \\ A_5=4\left[C_3\left(C_{11}+C_{21}\right)-2C_3C_4\sqrt{C_{11}C_3}\right]-C_{22}^2 \\ C_{11}=(\mu^2+1)\sin^4\theta \\ C_{21}=-\sin^2\theta \\ C_{22}=\sin^2\theta\left[2c\mu+2\cos^2\theta\left(\mu^2+1\right)\sigma_2+2\left(\mu^2\sin^2\theta-\cos^2\theta\right)\sigma_3\right] \\ C_3=\left[c+\mu\left(\sigma_2\cos^2\theta+\sigma_3\sin^2\theta\right)\right]^2-\left(\sigma_2-\sigma_3\right)^2\sin^2\theta\cos^2\theta \\ C_4=\dfrac{c_{t_0}}{{\sigma_{cl}}^2\sqrt{\mu^2+1}}\left[\csc^2\theta+\dfrac{\mu\sigma_{cl}+c_{t_0}\csc^2\theta}{\sqrt{\left(c_{t_0}+\mu\sigma_{cl}\sin^2\theta\right)^2-{\sigma_{cl}}^2\sin^2\theta\cos^2\theta}}\right] \end{cases}$$

It is observed from Eq. (31) that $\left(\sigma_1-\sigma_3\right)$ is related to the friction coefficient μ, the coefficient κ of mixed-mode fracture criterion, the long-term uniaxial compressive strength σ_{cl}, the short-term uniaxial tensile strength σ_t, the time factor $f_{in}(t_0)$, the dip angle of penny-shaped microcracks θ and Poisson's ratio ν.
Assumed that

$$\left(C_{11}+C_{21}\right)=0,C_{22}=s\sigma_{cl}+m\sigma_2-n\sigma_3,C_3=\left(s\sigma_{cl}+m\sigma_2-n\sigma_3\right)^2$$

Eq.(31) can be simplified to:

$$\left(\sigma_1-\sigma_3\right)^3+\left(s\sigma_{cl}+m\sigma_2-n\sigma_3\right)\left(\sigma_1-\sigma_3-s\sigma_{cl}\right)^2-s\sigma_{cl}\left(s\sigma_{cl}+m\sigma_2-n\sigma_3\right)^2=0 \tag{32}$$

where s,n and m are the strength parameters which are determined by experiments.

When Eq.(32) is expressed by the short-term uniaxial compressive strength σ_c, Eq.(32) can be rewritten as

$$\begin{aligned}&(\sigma_1-\sigma_3)^3+\left(\frac{s\sigma_c\sqrt{f_{iu}(0)}}{\sqrt{f_{iu}(t_0)}}+m\sigma_2-n\sigma_3\right)\\&\left(\sigma_1-\sigma_3-\frac{s\sigma_c\sqrt{f_{iu}(0)}}{\sqrt{f_{iu}(t_0)}}\right)^2-\frac{s\sigma_c\sqrt{f_{iu}(0)}}{\sqrt{f_{iu}(t_0)}}\left(\frac{s\sigma_c\sqrt{f_{iu}(0)}}{\sqrt{f_{iu}(t_0)}}+m\sigma_2-n\sigma_3\right)^2=0\end{aligned}\tag{33}$$

where σ_c is the short-term uniaxial compressive strength.

COMPARISON WITH THE EXPERIMENTAL RESULTS

The Lode stress angle is defined as follows:

$$\phi_\sigma=\arctan\left[\frac{2\sigma_3-(\sigma_1+\sigma_2)}{\sqrt{3}(\sigma_1+\sigma_2)}\right]\qquad(-30^0\le\phi_\sigma\le30^0)\tag{34}$$

The stress tensor σ_{ij} expressed by the first invariant I_1 of stress tensor and the second invariant of deviatoric stress tensor J_2 can be written as follows:

$$\begin{bmatrix}\sigma_1\\\sigma_2\\\sigma_3\end{bmatrix}=\frac{2}{\sqrt{3}}\sqrt{J_2}\begin{bmatrix}\sin(\phi_\sigma+\frac{2}{3}\pi)\\\sin(\phi_\sigma)\\\sin(\phi_\sigma-\frac{2}{3}\pi)\end{bmatrix}+\begin{bmatrix}I_1/3\\I_1/3\\I_1/3\end{bmatrix}\tag{35}$$

Micromechanics-based three-dimensional long-term strength criterion (32) can be expressed by the first invariant I_1 of stress tensor and the second invariant of deviatoric stress tensor J_2, the following expression can be obtained

$$F=f_1'q^3+f_2'pq^2+f_3'q^2+f_4'pq+f_5'p^2+f_6'q+f_7'p=0\tag{36}$$

where

$$\begin{cases}f_1'=\frac{4}{3}\cos^2\phi_\sigma\left[3(2+n)\cos\phi_\sigma+\sqrt{3}(2m+n)\sin\phi_\sigma\right]\\f_2'=4(m-n)\cos^2\phi_\sigma\\f_3'=\frac{1}{3}s\sigma_{cl}\left\{-2\left[-3+m^2+(3+m)n+n^2\right]+\left[6+2m^2+2mn-n(6+n)\right]\cos2\phi_\sigma-\sqrt{3}(2+n)(2m+n)\sin2\phi_\sigma\right\}\\f_4'=-\frac{2}{3}(m-n)s\sigma_{cl}\left[3(2+n)\cos\phi_\sigma+\sqrt{3}(2m+n)\sin\phi_\sigma\right]\\f_5'=-(m-n)^2s\sigma_{cl}\\f_6'=-\frac{1}{3}s^2\sigma_{cl}{}^2\left[3(4+n)\cos\phi_\sigma+\sqrt{3}(2m+n)\sin\phi_\sigma\right]\\f_7'=(-m+n)s^2\sigma_{cl}{}^2\end{cases}$$

$$p = I_1 / 3,\ q = \sqrt{J_2}$$

Similarly, Micromechanics-based three-dimensional long-term strength criterion (33) can be rewritten in another form:

$$F = f_1 q^3 + f_2 pq^2 + f_3 q^2 + f_4 pq + f_5 p^2 + f_6 q + f_7 p = 0 \tag{37}$$

where

$$\begin{cases} f_1 = \dfrac{4}{3}\cos^2\phi_\sigma\left[3(2+n)\cos\phi_\sigma + \sqrt{3}(2m+n)\sin\phi_\sigma\right] \\ f_2 = 4(m-n)\cos^2\phi_\sigma \\ f_3 = \dfrac{1}{3}s\sqrt{\dfrac{f_{iu}(0)}{f_{iu}(t_0)}}\sigma_c\left\{-2\left[-3+m^2+(3+m)n+n^2\right]+\left[6+2m^2+2mn-n(6+n)\right]\cos 2\phi_\sigma - \sqrt{3}(2+n)(2m+n)\sin 2\phi_\sigma\right\} \\ f_4 = -\dfrac{2}{3}(m-n)s\sqrt{\dfrac{f_{iu}(0)}{f_{iu}(t_0)}}\sigma_c\left[3(2+n)\cos\phi_\sigma + \sqrt{3}(2m+n)\sin\phi_\sigma\right] \\ f_5 = -(m-n)^2 s\sqrt{\dfrac{f_{iu}(0)}{f_{iu}(t_0)}}\sigma_c \\ f_6 = -\dfrac{1}{3}s^2\dfrac{f_{iu}(0)}{f_{iu}(t_0)}{\sigma_c}^2\left[3(4+n)\cos\phi_\sigma + \sqrt{3}(2m+n)\sin\phi_\sigma\right] \\ f_7 = (-m+n)s^2\dfrac{f_{iu}(0)}{f_{iu}(t_0)}{\sigma_c}^2 \end{cases}.$$

COMPARISON WITH THE EXPERIMENTAL DATA OF COAL

Series of triaxial compressive experimental data were obtained from creep tests on various rocks by Refs [25-27]. The long-term uniaxial compressive strength of rocks and the fitting strength parameters are listed in Tab. 1. Tabs. 2-4 show theoretical strength and the experimental data of Barre granite, Inada granite and Jinping marble. Figs 5-7 show that comparison of predicted strength and the experimental data of Barre granite, Inada granite and Jinping marble. It is found from Tabs 2-4 and Figs 5-7 that the proposed long-term strength criterion agrees well with experimental data of different rocks.

Rocks	The strength parameter(s)	The fitting strength parameter(m)	The fitting strength parameter (n)	Long-term uniaxial compressive strength	Reference
Barre granite	1	6.709	0.737	158	Kranz [25]
Inada granite	1	1.000	0.101	216	Maranini and Brignoli [26]
Jinping marble	1	12.184	18.566	80	Yang et al. [27]

Table 1: The fitting strength parameters and uniaxial compressive strength of different rocks.

σ_1(MPa)	σ_2(MPa)	σ_3(MPa)	q (MPa)	$p_{experimental}$ (MPa)	$p_{theoretical}$ (MPa)
280	10	10	270.000	100.000	99.255
289	10	10	279.000	103.000	102.245
298	10	10	288.000	106.000	103.266
301	10	10	291.000	107.000	104.614
304	10	10	294.000	108.000	105.966
306	10	10	296.000	108.667	106.869
312	10	10	302.000	110.667	109.587
315	10	10	305.000	111.667	110.952
494	40	40	454.000	191.333	193.264
468	40	40	428.000	182.667	180.006
369	20	20	349.000	136.333	131.381
288	10	10	278.000	102.667	98.800
247	5	5	242.000	85.667	85.051
234	5	5	229.000	81.333	77.492
280	10	10	270.000	100.000	102.255
289	10	10	279.000	103.000	99.245
298	10	10	288.000	106.000	103.266
301	10	10	291.000	107.000	104.614

Table 2: Theoretical strength and the experimental data of Inada granite.

σ_1(MPa)	σ_2(MPa)	σ_3(MPa)	q (MPa)	$p_{experimental}$ (MPa)	$p_{theoretical}$ (MPa)
162.1	0.1	160	270	100.0000	106.415
173.1	0.1	230	279	103.0000	103.952
177.1	0.1	220	288	106.0000	105.514
179.1	0.1	110	291	107.0000	101.884
185.1	0.1	180	294	108.0000	108.765
188.1	0.1	205	296	108.6667	104.870
196.1	0.1	235	302	110.6667	109.826
199.1	0.1	249	305	111.6667	112.323
203.1	0.1	223	454	191.3333	194.439
262	10	262	428	182.6667	183.837
343	25	100	349	136.3333	135.572
348	53	350	278	102.6667	107.943

Table 3: Theoretical strength and the experimental data of Barre granite.

σ_1(MPa)	σ_2(MPa)	σ_3(MPa)	q (MPa)	$p_{experimental}$ (MPa)	$p_{theoretical}$ (MPa)
110	20	12	94.255	47.333	45.757
120	20	14	103.131	51.333	52.277
130	20	18	111.014	56.000	58.335
140	20	20	120.000	60.000	59.550
150	20	20	130.000	63.333	63.965
160	20	20	140.000	66.667	65.786
170	20	20	150.000	70.000	72.013
155	35	35	120.000	75.000	75.550
165	35	35	130.000	78.333	77.965
175	35	35	140.000	81.667	82.786
185	35	35	150.000	85.000	86.013
195	35	35	160.000	88.333	89.647
205	35	35	170.000	91.667	91.687
215	35	35	180.000	95.000	92.134
180	50	45	132.571	91.667	96.193
190	50	47	141.524	95.667	94.165
200	50	46	152.040	98.667	93.945
210	50	50	160.000	103.333	101.647
220	50	50	170.000	106.667	101.687
230	50	50	180.000	110.000	112.134

Table 4: Theoretical strength and the experimental data of Jinping marble.

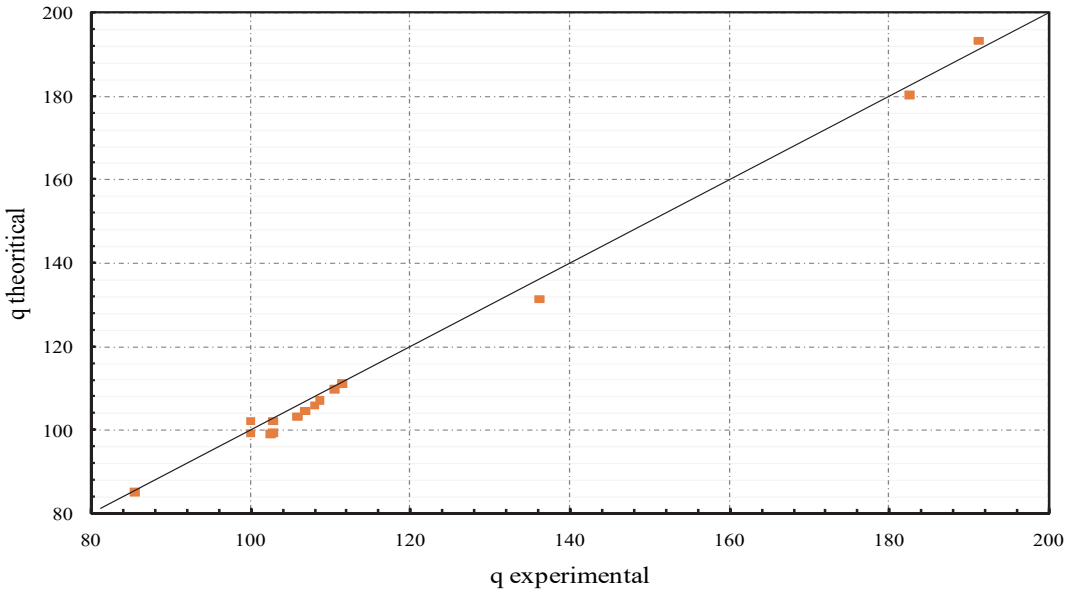

Figure 5: Comparison of predicted strength and the experimental data of Inada granite.

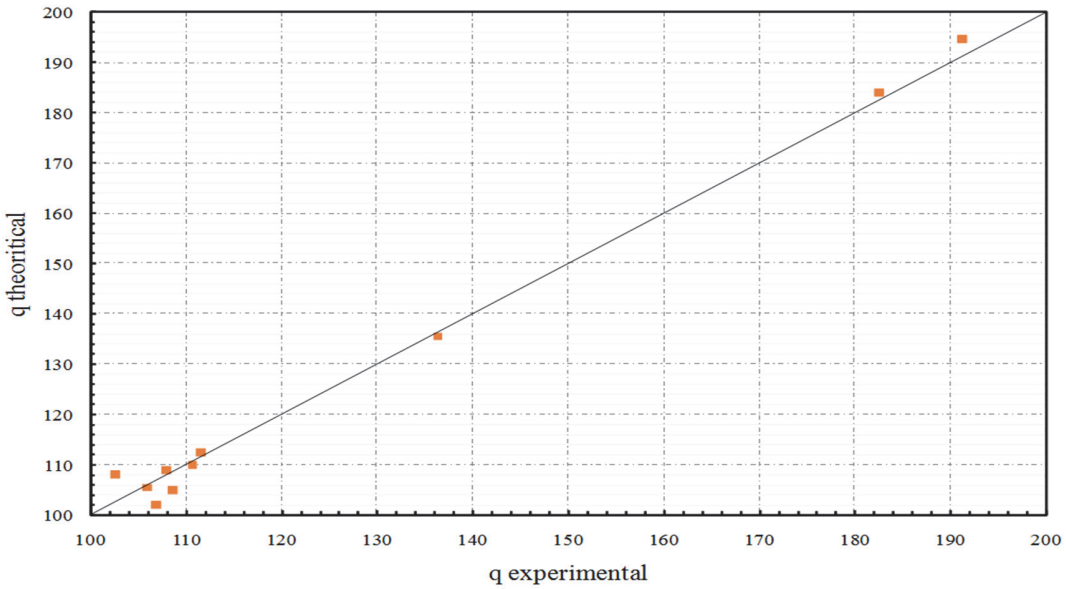

Figure 6: Comparison of predicted strength and the experimental data of Barre granite.

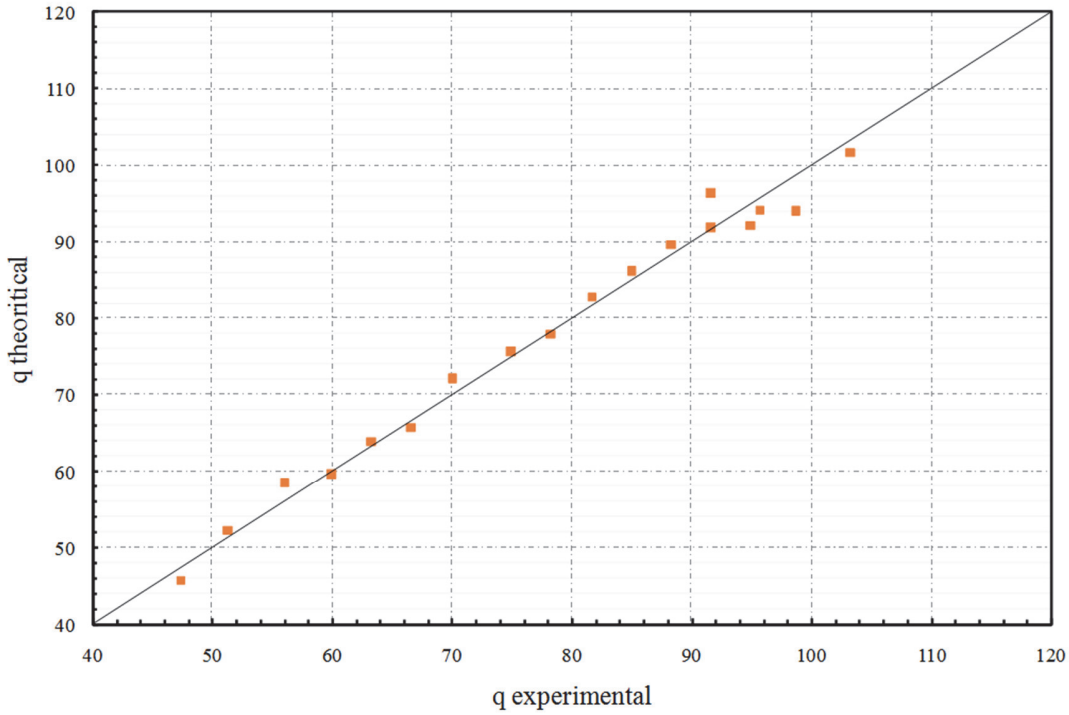

Figure 7: Comparison of predicted strength and the experimental data of Jinping marble

Discussions and Conclusions

In this paper, Burgers model with the characteristics of instantaneous elastic deformation, primary creep and steady-rate creep is applied to investigate creep fracture behaviors of penny-shaped microcracks. Mode II stress intensity factor at tips of three-dimensional penny-shaped microcracks embedded in Burgers viscoelastic rock matrix is derived. The orientation angle of micro-failure in Burgers viscoelastic rocks is defined. A novel micromechanics-based three-dimensional long-term strength criterion is proposed to investigate effects of time and the intermediate principal stress on

the creep failure of rocks. By comparison with the previous experimental results, it is found that the novel micromechanics-based three-dimensional long-term strength criterion is in good agreement with experimental data.

ACKNOWLEDGMENTS

This work was supported by the National Natural Science Foundation of China (Nos. 51325903 and 51679017), project 973 (Grant no. 2014CB046903), Graduate Scientific Research and Innovation foundation of Chongqing, China (Grant No. CYB16012), Open Research Fund Program of Hunan Provincial Key Laboratory of Geotechnical Engineering for Stability Control and Health Monitoring, Natural Science Foundation Project of CQ CSTC (Nos. cstc2013kjrc-ljrccj0001 and cstc2013jcyjys0005) and Research fund by the Doctoral Program of Higher Education of China(No.20130191110037).

REFERENCES

[1] Baud, P. and Meredith, P. G., (1997). Damage accumulation during triaxial creep of darley dale sandstone from pore volumometry and acoustic emission, Int. J. Rock Mech. Min. Sci. 34, pp. 24.e1–24.e10.
[2] Heap, M. J., Baud, P., Meredith, P. G., Bell A. F. and Main, I.G., (2009). Time-dependent brittle creep in Darley Dale sandstone, J. Geophys. Res.D: Atmos, 114, pp. 1–22.
[3] Heap, M. J., Baud, P., Meredith, P. G., Vinciguerra, S., Bell, A. F. and Main, (2011). I.G., Brittle creep in basalt and its application to time-dependent volcano deformation, Earth Planet Sci. Lett., 307, pp. 71–82.
[4] Li, Y. and Xia, C., (2000). Time-dependent tests on intact rocks in uniaxial compression, Int. J. Rock Mech. Min. Sci., 37, pp. 467-475.
[5] Shin, K., Okubo, S., Fukui, K. and Hashiba, K., (2005). Variation in strength and creep life of six Japanese rocks, Int. J. Rock Mech. Min. Sci., 42, pp. 251-260.
[6] Aubertin, M., Li, L. and Simon, R., (2000). A multiaxial stress criterion for short- and long-term strength of isotropic rock media, Int. J. Rock Mech. Min. Sci., 37, pp. 1169-1193.
[7] Amitrano, D. and Helmstetter, A., Brittle creep, damage and time to failure in rocks, (2006). J. Geophys. Res. B: Solid Earth, 111, pp. 335-360.
[8] Bahaaddini, M., Hagan, P.-C., Mitra, R. and Hebblewhite, B.-K., (2015). Numerical Study of the Mechanical Behavior of Nonpersistent Jointed Rock Masses, Int. J. Geomech., 10.1061/(ASCE)GM.1943-5622.0000510, 04015035.
[9] Barla, M. and Beer, G., (2012). Special Issue on Advances in Modeling Rock Engineering Problems, Int. J. Geomech., 12, pp. 617-617.
[10] Yang, Q., Chen, X. and Zhou, W. Y., (2005). On the structure of anisotropic damage yield criteria, Mech. Mater., 37, pp. 1049-1058.
[11] Zhou, X. P., Bi J. and Qian, Q. H., (2015). Numerical simulation of crack growth and coalescence in rock-like materials containing multiple pre-existing flaws, Rock Mech. and Rock Eng., 48, pp. 1097-1114.
[12] Zuo, J. P., Li, H. T., Xie, H. P., Ju, Y. and Peng, S. P., (2008). A nonlinear strength criterion for rock-like materials based on fracture mechanics, Int. J. Rock Mech. Min. Sci., 45, pp. 594-599.
[13] Al-Ajmi, A. M. and Zimmerman, R. W., (2005). Relation between the mogi and the coulomb failure criteria, Int. J. Rock Mech. Min. Sci. 42, pp. 431–439.
[14] Paterson, M. S. and Wong, T. F., (2005). Experimental rock deformation - the brittle field, Mineral Mag., 43, pp. 163-186.
[15] Yu, S. W. and Feng, X. Q., (1995). A micromechanics-based damage model for microcrack-weakened brittle solids, Mech. Mater., 20, pp. 59-76.
[16] Tada, H., (1973). The stress analysis of cracks handbook, Stress Analysis of Cracks Handbook, 91, pp. 614.
[17] Yi, S. M. and Zhu, Z.D., (2005). Introduction to damage mechanics of crack-weakened rock masses, Science Press, Beijing.
[18] Zhou, Z. B., (1983). Stress intensity factors for creep fracture and their application, Acta Mech. Solida Sin., 1, pp. 100-104.
[19] Erdogan, F. and, Sih, G. C., (1963). On the crack extension in plates under plane loading and transverse shear, J. Basic Eng. Asme, 85, pp. 527.

[20] Aboudi, J. and Benveniste, Y., (1987). The effective moduli of cracked bodies in plane deformations, Eng. Fract. Mech., 26, pp. 171-184.

[21] Budiansky, B. and O'Connell, R. J., (1976). Elastic moduli of a cracked solid ☆. Int. J. Solids Struct., 12, pp. 81-97.

[22] Kachanov, M., (1992). Effective elastic properties of cracked solids: critical review of some basic concepts, Appl. Mech. Rev., 45, pp. 304-335.

[23] Paterson, M. S. and Wong, T. F., (2005). Experimental rock deformation - the brittle field, Mineral Mag., 43, pp. 163-186.

[24] Brady, B. T., (1969). A statistical theory of brittle fracture for rock materials Part II—brittle failure under homogeneous triaxial states of stress, Int. J. Rock Mech. Min. Sci. Geomech. Abstr., 6, pp. 285-300.

[25] Kranz, R. L., (1980). The effects of confining pressure and stress difference on static fatigue of granite, J. Geophys. Res.D: Atmos, 85, pp. 1854-1866.

[26] Maranini, E. and Brignoli, M., (1999). Creep behaviour of a weak rock. experimental characterization, Int. J. Rock Mech. Min. Sci., 36, pp. 127-138.

[27] Yang, S. Q., Xu, P., Ranjith, P. G., Chen, G. F. and Jing, H. W., (2015). Evaluation of creep mechanical behavior of deep-buried marble under triaxial cyclic loading, Arab. J. Geosci., pp. 81-16.